MICROTREMOR COHERENCY: SIMULTANEOUS RECORDING WITH ARRAYS HAVING DIFFERENT APERTURES

W. R. Stephenson[1]

SUMMARY

By recording microtremors simultaneously using arrays having two apertures, the effect of incoherent noise, which can act to depress coherency values, may be reduced, leading to better estimates of azimuthally-averaged coherency, and hence to improved shear-wave velocity profiles at sites. The method is exemplified by the use of 30 m and 40 m triangular arrays at McEwan Park, Lower Hutt, New Zealand, where the method is shown to result in better fits to theoretical coherency. Adequate correction is confined to low frequencies (less than 4.5 Hz in this case). Estimates of Vs are modified for greater depths (50 to 200m in this example) but unaltered for near-surface materials.

1 INTRODUCTION

An increasingly popular way to characterise the seismic response of an area is to use an array of seismographs to make simultaneous recordings of microtremors within the area and then to process the data in the domains of space and time under various assumptions, with the ultimate intention of obtaining a shear-wave velocity profile at the location of the array. In one implementation known as the SPAC (SPatial AutoCorrelation) method, values of azimuthally-averaged coherency are obtained, and the shear-wave velocity profile is determined by inverting these values. Using the SPAC method there are two main approaches to the inversion of the azimuthally-averaged coherencies.

In the first approach (typified by [1]) a trial model of the area which assumes plane layers of soil and incorporates guessed values for s-wave velocity, p-wave velocity and density for each layer, may have its theoretical coherency computed (under the assumption that the microtremors result from Rayleigh waves) and compared with the field value, so that the trial model may be altered iteratively until a good match between field coherency and theoretical coherency is achieved. In the second approach (typified by [2]) the coherency is inverted to become a Rayleigh-wave dispersion curve, which is in turn inverted to become a velocity profile.

Both these approaches have their merits. The single-step inversion has an inherent simplicity whereas the two-step inversion seems at first sight to accumulate the errors of two inversions. In fact the first inversion of the two-step process is nearly unique in that the only ambiguity concerns the periodic nature of Bessel functions, and the correct value can readily be obtained. In addition, the use of existing methods to invert dispersion curves can simplify the second inversion of the two-step process.

Using either approach, any complete treatment of the array measurements has to acknowledge that the signal recorded at each instrument location is a superposition of amplifier noise, body waves and surface waves. Either type of wave in turn may be plane or non-plane. As a consequence, either of the two approaches outlined above must make simplifying assumptions regarding the nature of the ground motion measurements. These assumptions vary according to the particular method chosen, but it is usual to assume no instrumentation noise, no body waves and no Love waves (by considering only vertical motion). In other words it is assumed that only various modes of Rayleigh waves, both plane and non-plane, are involved.

It is most usual to assume that only fundamental-mode Rayleigh waves traverse the array, and good results are often obtained under this assumption. However it has been shown [3] that for some array dimensions, some portions of the coherency curve can be better explained by considering higher modes of Rayleigh wave.

It is well recognised that field coherency curves incorporate all vertical ground motion whereas the theoretical coherency curves concern only plane surface waves. There have been attempts e.g. [4] to treat non-plane surface waves due to local sources but there do not appear to be any explicit treatments of signals that arise from sources other than surface waves. These could for instance be vertically-propagating plane waves, extremely local sources or amplifier noise. Whatever their origin, they have one feature in common; they must act to depress the amplitude of the field coherency that would arise from plane surface waves alone. This is because the coherency is defined as the normalised cross-power spectrum, the normalisation being the process of dividing the cross-power spectrum by the total power spectrum. It follows that unless the recorded motion consists entirely of surface waves, the only frequencies for which the values of coherency will be accurate will be at the zero crossovers. At all other frequencies the coherency values will have a smaller magnitude than would be the case for purely surface-wave motion. Signals which are identical for all array members, such as for vertically arriving p-waves, will increase the coherency at all frequencies as well as depressing coherencies due to waves traversing the array. These aspects are well explained in [5].

2. A STRATEGY FOR COUNTERING UNWANTED SIGNALS

The most obvious way of diminishing incoherent noise while still retaining coherent signals, is to record the microtremors for longer. This is because coherent signals rise linearly with

[1] *Scientist, GNS Science, PO Box 30368, Lower Hutt, New Zealand*

time while incoherent signals ideally rise with the square root of time [6]. However this approach can be operationally expensive. The noise-compensated CCA method [7] offers a different alternative but requires a circle of recorders with a central member.

If microtremors were recorded at a site with arrays that had apertures that increased in small steps it would be possible to implement a noise-free matching scheme that only used zero crossings of the coherency curves, but this would be expensive in either time or number of instruments required.

The fact that the azimuthally-averaged coherencies for two different array apertures at a site will be quite different, but will include the same incoherent noise at each frequency, suggests a different approach.

Suppose that for a given site, two SPAC arrays with different apertures are set up. Normally for each array we would write

$$C = J_0(2\pi fd/v(f)) \quad (1)$$

where

C is the azimuthally-averaged coherency,
J_0 is a zero-order Bessel function,
f is the frequency of the Rayleigh wave
d is the aperture of the array, and
$v(f)$ is the velocity of the Rayleigh wave (a function of frequency)

If only a constant proportion, say $k(f)$, of the signal at each member of each array consists of surface waves, the coherency will fall, being multiplied by a factor $k(f)$ which is less than 1, such that the coherencies for the two arrays will become

$$C_1 = k(f)J_0(2\pi fd_1/v(f)) \quad (2)$$

for array 1 which has an aperture d_1 and

$$C_2 = k(f)J_0(2\pi fd_2/v(f)) \quad (3)$$

for array 2 which has an aperture d_2

Equations (2) and (3) are a pair of simultaneous equations in two unknowns and accordingly it should be possible to solve them for k and v at each frequency. Note that both k and v are functions of f. Once $k(f)$ has been determined the way to proceed would be to divide the field coherency (for either array) by $k(f)$ thus obtaining more correct coherencies. After doing this the steps taken to arrive at a shear-wave profile could be those normally taken for a single array.

3 THE MCEWAN PARK SITE

For some years, McEwan Park, near the estuary of the Hutt river, Wellington, New Zealand (Figure 1), has proven to be a useful test site for investigating non-invasive site-characterisation techniques. This usefulness arises because the site is simple, is clear of buildings, has been investigated with a variety of techniques, and is easy of access. For these reasons, McEwan Park was chosen to evaluate the usefulness of the procedure outlined previously.

The simplicity of the site arises because of the processes that led to its formation. In broad terms, a tectonically-formed basin was filled with layers of alluvium during four glacial and four interglacial regimes starting 1.8 Ma ago. With the passage of time, and under the compression of overlying layers, the lower materials have become consolidated and stiffened, and so constitute a contrasting basement to the upper 21m of Holocene sands, silts and clays which are young and flexible.

The McEwan Park site is described in [8], which gives a comprehensive account of the origin and properties of the materials underlying McEwan Park, relying on a seismic cone

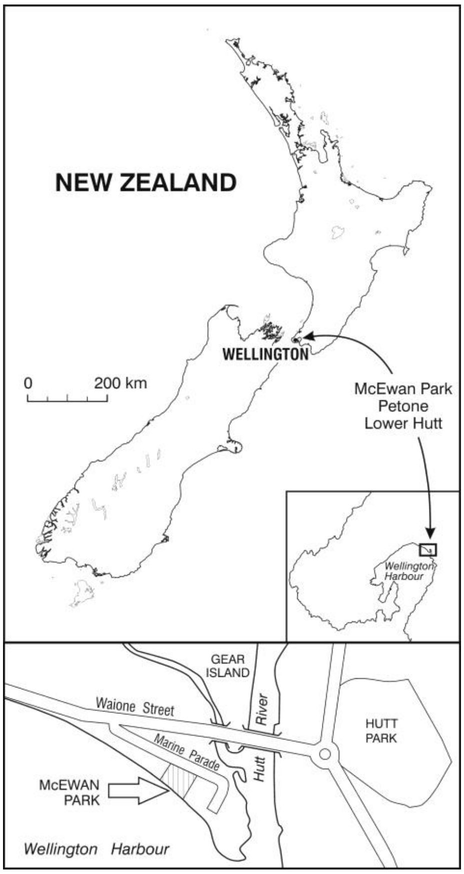

Figure 1: ***Location diagram showing McEwan Park.***

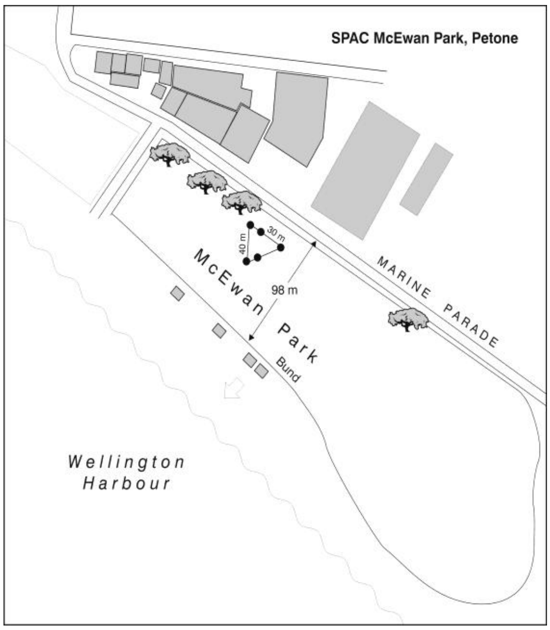

Figure 2: ***Layout of the McEwan Park microtremor array. Five seismographs were operated at a time, allowing simultaneous recordings***

penetration test (SCPT) to assign a shear-wave velocity of 160 m/s and a thickness of 21 m to the Holocene deposits, and a seismic refraction test to assign a shear-wave velocity of 525 m/s to the top part of the underlying materials. Details of the properties and thickness of the full column of underlying materials are uncertain, but a velocity greater than 500 m/s and a thickness of the order of 200 m are reasonable. Figure 3 shows how the SCPT and refraction tests define the shear-wave velocity profile.

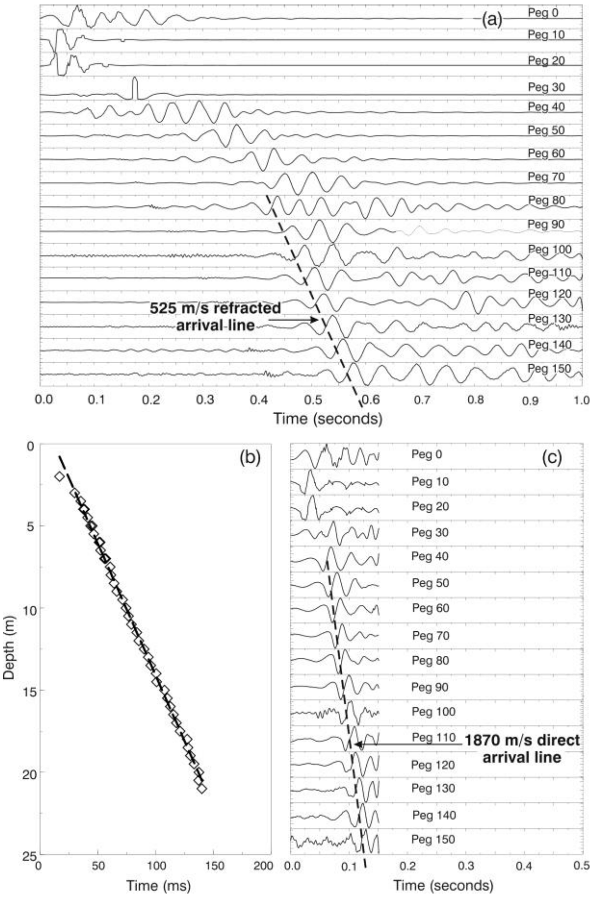

Figure 3: ***Site conditions at McEwan Park. (a) Radial arrivals from seismic refraction test, showing that the gravels below 21 m have an s-wave velocity of 525 m/s. (b) Shear-wave arrivals versus depth from SCPT test, showing an s-wave velocity of 160 m/s in the estuarine materials. (c) Vertical arrivals from seismic refraction test, showing that the estuarine materials have a p-wave velocity of 1870 m/s.***

It has been shown [4] that a triangular array provides a sufficient estimate of coherency at low frequencies, with a hexagonal array providing better results for a dominant close source of microtremors. However in the case of the plane waves likely to be incident at the McEwan Park site (an arterial highway some 250 m away is presumed to be the dominant source of microtremors) a regular hexagonal array and an equilateral triangular array will give the same coherencies because only three independent inter-station directions are involved. Accordingly five seismographs (Nanometrics Taurus with Lennartz LE-3Dlite 1Hz sensors) were laid out on McEwan Park to form two equilateral triangles with sides of 30 m and 40 m, with one recorder common to both triangles as shown in Figure 2. Microtremors were recorded for half an hour, and azimuthally-averaged coherencies calculated for the two triangles. These coherencies are shown in Figure 4 and Figure 5, together with the coherencies expected for fundamental-mode Rayleigh waves travelling in an infinitely-extended geometry based on the known and inferred properties of the materials underlying McEwan Park. These properties were:

Thickness (m)	P-velocity (m/s)	S-velocity (m/s)	Density (t/m^3)
21.0	1500.0	160.0	1.8853
150.0	1500.0	525.0	2.1040

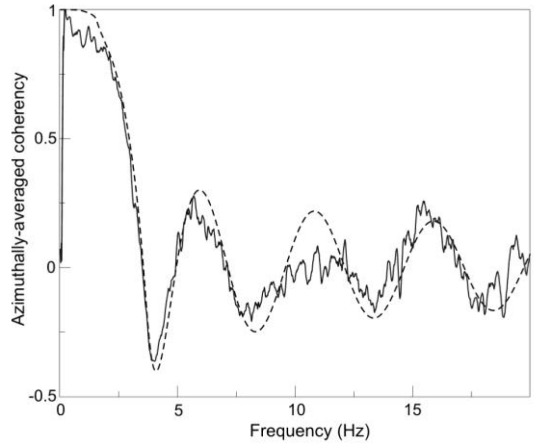

Figure 4: ***Azimuthally-averaged coherency of vertical motion (solid line) for a triangular array of 30 m aperture, together with the value expected (dashed line) for the known shear-wave velocity profile at the McEwan Park site.***

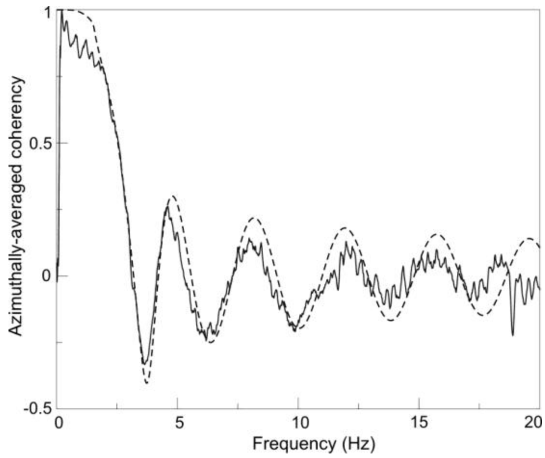

Figure 5: ***Azimuthally-averaged coherency of vertical motion (solid line) for a triangular array of 40 m aperture, together with the value expected (dashed line) for the known shear-wave velocity profile at the McEwan Park site.***

The basis of choosing a p-wave velocity was to assume 1.73 times the s-wave velocity, with a minimum of 1500 m/s (the velocity of sound in water). This is in contrast to the measured value of 1870 m/s shown in Fig 3, but was adopted because the accuracy of Fig 3 is limited, and small changes in p-wave velocity play a minor role in determining Rayleigh wave characteristics. The basis of choosing a density was to take a value of 2.2-50/Vs.

Properties of the underlying rock were assumed to be

Thickness (km)	P-velocity (km/s)	S-velocity (km/s)	Density (t/m^3)
0.4	4.3942	2.54	2.1803
4.6	5.4668	3.16	2.1842
10	6.0377	3.49	2.1857
10	6.0550	3.5	2.1857
10	6.7816	3.92	2.1872
10	8.3178	4.808	2.1896
Half space	8.4078	4.86	2.1897

The rock p-wave and s-wave velocity values were taken from http://www.geonet.org.nz/resources/earthquake/hypocentre-derivation.html.

The expected coherencies were obtained by using existing software routines [9] based on a matrix propagator approach. Figures 4 and 5 have some noteworthy features. As expected, the trace for the 40 metre aperture array oscillates more rapidly than does the trace for the 30 metre aperture array. Values for field coherency are generally depressed below the theoretical values. Zero crossings for field and theoretical coherencies are at the same frequencies.

These observations are in accordance with the model adopted being accurate, and they are consistent with fundamental-mode Rayleigh waves dominating the microtremor field, but with a small amount of incoherent noise also being present.

4 CORRECTING MCEWAN PARK COHERENCIES

A convenient way to solve equations (2) and (3) is to divide (2) by (3), thus eliminating $k(f)$, but leaving a somewhat complicated expression for $v(f)$.

$$C_1/C_2 = J_0\,(2\pi\, fd_1/v(f))\ /J_0\,(2\pi\, fd_2/v(f)) \qquad (4)$$

However equation (4) can be solved numerically for $v(f)$ at each frequency, and k found by substitution in (2) or (3). This study used Newton's method to solve (4). Corrected values were only sought above 0.49 Hz because it was thought that below this frequency corrections would be meaningless as they would be overwhelmed by errors arising from the small size of the array aperture. An initial value for $v(f)$ of 1000 m/s at low frequency was taken, and at successively higher frequencies the previous solution for $v(f)$ was taken as an initial value to ensure quick convergence. This strategy proved successful except at near-zero values of C_2. In order to circumvent this, and to verify the value of $k(f)$, the alternative expression, equation (5), was solved by the same method and the values of $k(f)$ combined.

$$C_1/C_2 = J_0\,(2\pi\, fd_2/v(f))\ /J_0\,(2\pi\, fd_1/v(f)) \qquad (5)$$

The combination of correction factors was achieved by plotting both versions on the same graph as shown in Figure 6, and limiting the frequency range to values for which either there was agreement, or one value was near zero (because of the numerical instability). Outside this range (0.49 Hz to 4.59 Hz) the factor was assumed to be unity. Within the acceptable range the value was normally taken as the mean of the two versions, but if one version was zero the other version was adopted. The result is shown in Figure 7.

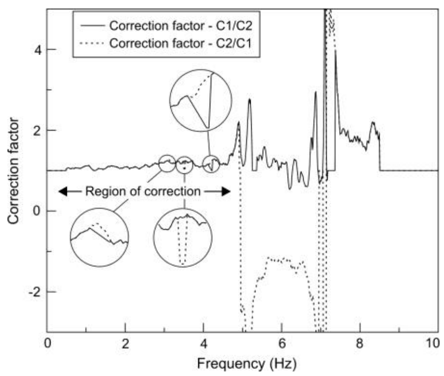

Figure 6: ***Correction factors derived from the coherencies, assuming that a constant amount of incoherent noise is present at each recorder. The correction factor is the inverse of k(f). Two methods were used because of numerical instabilities, one plotted as a solid, and the other as a dashed. line. Insets are 5x enlargements of the regions where one of the methods became unstable as the relevant coherency approached zero. Below 4.6 Hz the most appropriate value was selected but above 4.6 Hz the correction process was considered to be unreliable because the two methods gave inconsistent results.***

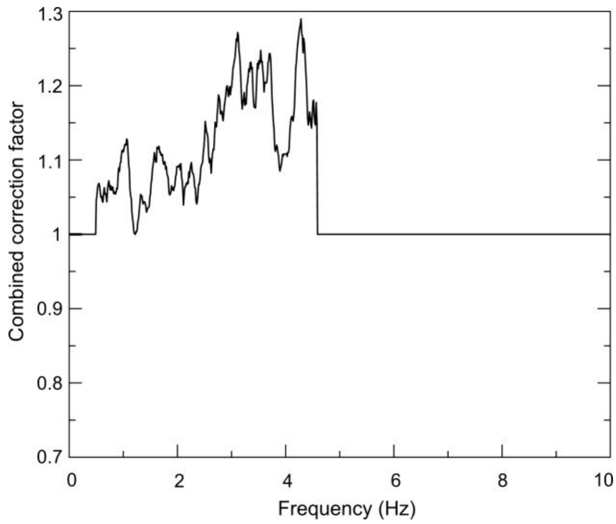

Figure 7: ***Combined correction factor which was adopted.***

At this point it is worthwhile re-stating the assumptions that were made when devising this method. The original basis was the existence at any frequency of signals that contribute to the geometric mean of the autocorrelations of a pair of stations without contributing to the cross correlation between the pair of stations. Random noise associated with each sensor/digitiser package would behave this way, and a possible example is digitising noise. Even though the resolution of a digitiser may seem small compared with the mean signal amplitude it can still decrease the signal to noise ratio at low frequencies because ground motion signals fall off with a decrease in frequency, particularly when the transducer senses ground acceleration or velocity.

A signal source close to one of the sensors can also diminish the coherency between two stations. Such a signal may be derived for instance from wind acting on a cable or a nearby tree, water flowing in a nearby pipe, or close traffic, vehicle or pedestrian.

Other non-Rayleigh-wave signals can also perturb coherencies, but in ways which would need to be countered by different strategies. An example is body waves which may be incident vertically or obliquely at a site, affecting all sensors of an array. In the case of vertical or near-vertical incidence such plane waves would induce an offset in the coherency at frequencies contained in the body wave. Such an offset would be a function of frequency.

Once a corrected coherency curve has been obtained it may be inverted by either of the two strategies outlined towards the end of section 1.

5 EFFECTS ON CALCULATED DISPERSION

The work described so far has shown that using the two-aperture correction technique results in small improvements to coherencies. This is seen by comparing Figure 4 with Figure 8 and Figure 5 with Figure 9. It is however relevant to know whether these improvements would be reflected in significant changes to the calculated dispersion or to the calculated shear-wave velocity profile.

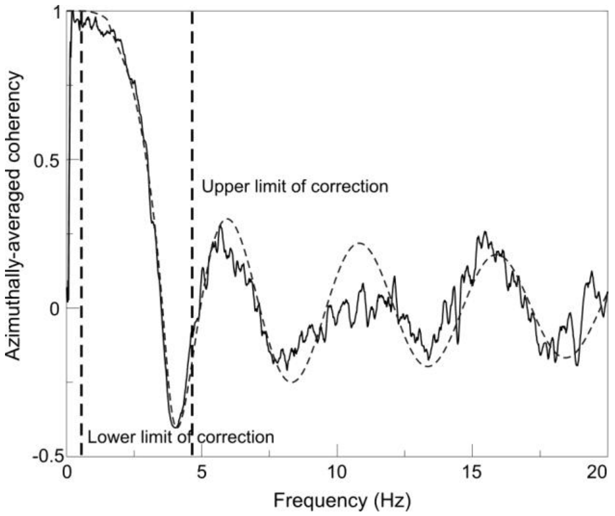

Figure 8: ***Azimuthally-averaged coherency for the 30 m array, when corrected, (solid line) and theoretical values (dashed line). Note that the peaks are now much closer in amplitude to the expected peaks, and coherencies for low frequencies approach closer to unity.***

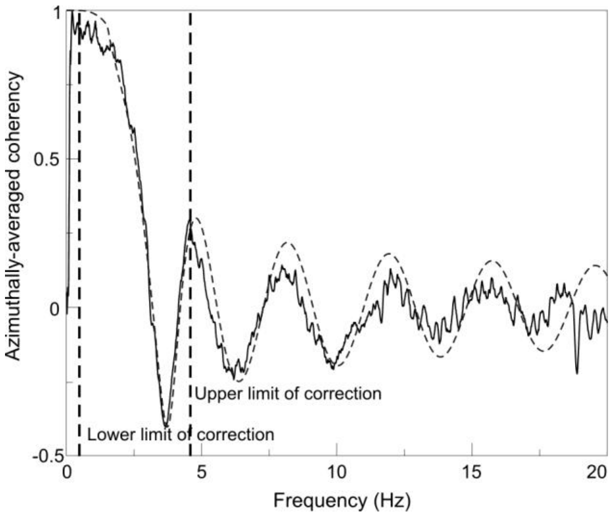

Figure 9: ***Azimuthally-averaged coherency for the 40 m array, when corrected, (solid line) and theoretical values (dashed line). Note that the peaks are now much closer in amplitude to the expected peaks, and coherencies for low frequencies approach closer to unity.***

It is a relatively trivial matter to invert the corrected and uncorrected coherencies into their equivalent dispersions, and this has been performed for the McEwan Park results by simply stepping the velocity at 1 m/s intervals in equation (1), recording the zero transitions of calculated velocity, and amalgamating the results into a single dispersion curve. It should be noted that the process of renormalising the coherencies assumes an identical velocity for both arrays at each frequency, so that although the uncorrected coherencies give rise to different velocities, the dispersion character for the corrected coherencies will be the same for both arrays. This proved to be the case when the corrected coherencies were plotted, lending some credence to the numerical procedures adopted.

The dispersions are shown in Figure 10 where there is a 20% difference in velocity at 2 Hz between the corrected results and the uncorrected results for the 40 m array. It is clear that the renormalisation procedure can significantly alter coherencies, and therefore change the velocity profile attributed to the site.

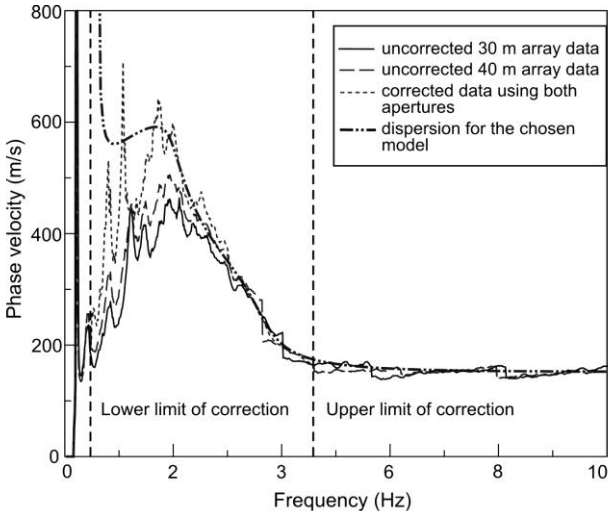

Figure 10: ***Phase velocity dispersion curves for the raw 30 m coherency (solid line) , for the raw 40 m coherency (dashed line), for the corrected coherency (dotted line) and for a model based upon corrected coherency (dot-dashed line). While the correction process made only a small difference to the coherency curve, it changed the dispersion curves significantly. This is because of the low slope of the coherency curve at low frequencies.***

However Figure 10 contains an equally important result. At frequencies below 1.7 Hz the phase velocities progressively decrease, eventually falling to improbably low values (as the frequency falls, it is usual for deeper and stiffer material to be sampled, and for the phase velocity to increase). Below 1.7 Hz the dispersion obtained from the corrected data, and the dispersion obtained from a credible model, differ substantially. This is presumably due to an interaction between the small gradient of J_0 (a zero-order Bessel function of the first kind) for small arguments, and errors in the coherency due to the input waveforms not being purely fundamental-mode Rayleigh waves. Thus it is unwise to use the correction process uncritically.

For example consider the case at 0.42 Hz, where the uncorrected coherency of 0.959 implies a velocity of 256 m/s. Had 4% of the coherency arisen from causes other than the passage of pure fundamental-mode Rayleigh waves, the true coherency would have been 0.997, and the appropriate velocity 1024 m/s.

For the frequency and aperture chosen above it is clear that small incoherent noise contributions to the signals recorded at the site may only produce small downward biases in the coherency but can result in large downward biases in estimated phase velocities. Note that this point is discussed in [10] when the difference between f-k processing (gives biases to high velocity) and SPAC processing (gives biases to low velocity) is treated.

6 EFFECTS ON CALCULATED VELOCITY PROFILE

At this stage it is evident that the correction process can improve estimates of azimuthally-averaged coherency and that there can be consequent changes in the shear wave dispersion characteristics. However from a practical viewpoint the shear wave velocity profile is of much greater concern, so the question is "what effect does the correction have on the shear-wave velocity profile". To answer this, the shear-wave velocity profiles for McEwan Park have been determined, before and after the correction procedure.

Trial-and-error matching in the frequency domain was chosen and the results are shown in Figure 11, where it is shown that the correction process changes the assigned properties of deeper material. Two profiles with equally-good matches to the corrected dispersion curve are shown in order to emphasise that the matching process becomes less reliable at depth, and that the correction merely implies generally greater velocities at depth.

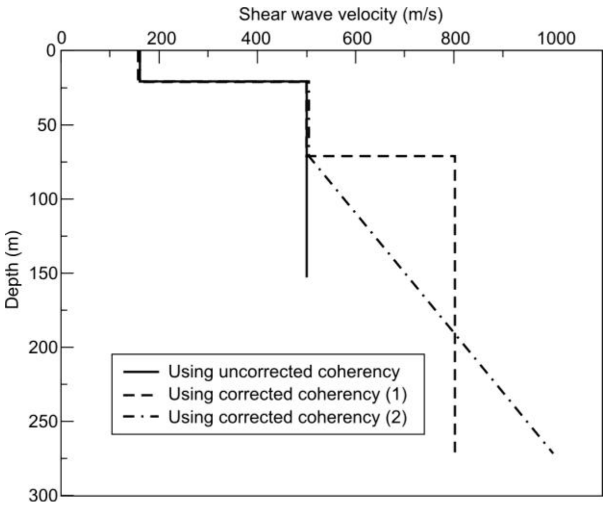

Figure 11: ***Shear wave velocity profiles derived from the uncorrected coherency (dashed lines) and the corrected coherency (solid line). Two equally-credible profiles are shown for the corrected dispersion.***

7 CONCLUSIONS

This study has shown on the basis of theory and of one example, that non-Rayleigh-wave components of microtremor array signals or random noise which are incoherent between array stations, will act to depress coherencies, but may be corrected for by the simultaneous use of two array apertures. The method is demonstrated here to be applicable to those frequencies below the first secondary maximum of the Jo curve.

ACKNOWLEDGMENTS

Michael Asten of Monash University, Melbourne, Australia, initiated microtremor studies at McEwan Park and subsequently encouraged the publication of the current study, making helpful suggestions. He also formally reviewed this paper. Peter Barker of Barker Consulting undertook the microtremor measurements used in this study, and was the major contributor to the site characterisation studies. Charlie O'Reilly of GNS Science carried out the seismic refraction tests, the results of which are contained in Figure 2. Thorough reviews by Graeme McVerry and Dick Beetham of GNS Science resulted in improvements to the text.

REFERENCES

1 Roberts, J.C. and Asten, M.W., (2005) "Estimating the shear velocity profile of Quaternary silts using microtremor array (SPAC) measurements" *Exploration Geophysics* (Melbourne), Vol. **36**, no. 1, pp.34-40

2 Chávez-García, F. J., Rodríguez, M., Stephenson, W. R. (2004) "Site effects and SPAC; results for three sites in Wainuiomata" *Bulletin of the New Zealand National Society for Earthquake Engineering*, Vol. **37**, no. 3, pp.101-110

3 Asten, M.W., Dhu, T., and Lam, N. (2004) "Optimised array design for microtremor array studies applied to site classification; observations, results and future use": Paper 2903, *Conference Proceedings of the 13th World Conference of Earthquake Engineering*, Vancouver, Aug 1-6, 2004

4 Roberts, J.C. and Asten, M.W. (2008) "A study of near source effects in array-based (SPAC) microtremor surveys" *Geophysical Journal International* **174**(1):159-177.

5 Cho, I., Tada, T. and Shinozaki, Y. (2008) "Assessing the applicability of the spatial autocorrelation method: A theoretical approach" *Journal of Geophysical Research* **113**(B6):B06307.

6 Tagare, P. (1993) "Signal averaging" Chapter 9 of Tompkins, W. *Biomedical digital signal processing*, Prentice-Hall.

7 Cho, I., Tada, T. and Shinozaki, Y. (2007) "Beyond the SPAC Method: Exploiting the Wealth of Circular-Array Methods for Microtremor Exploration" *Bulletin of the Seismological Society of America*, **97**(6):2080–2095.

8 Asten, M. W., Stephenson, W.R., and Davenport, P. N. (2005) "Shear-wave Velocity Profile for Holocene Sediments Measured from Microtremor Array Studies, SCPT, and Seismic Refraction" *Journal of Environmental & Engineering Geophysics* **10**(3): 235 – 242.

9 Herrmann, R.B. (2001) "Computer programs in seismology - an overview of synthetic seismogram computation Version 3.1: *Department of Earth and Planetary Sciences, St Louis Univ.*

10 Asten, M.W. and Boore, D.M. (2005) "Comparison of shear-velocity profiles of unconsolidated sediments near the Coyote borehole (CCOC) measured with fourteen invasive and non-invasive methods, in Asten, M.W. and Boore, D.M., eds., Blind comparisons of shear-wave velocities at closely spaced sites in San Jose, California: U.S. Geological Survey Open-File Report 2005-1169.